

Identification of mineralization features and deep geochemical anomalies using a new FT-PCA approach

Hossein Shahi^{*}, Reza Ghavami¹, Abolghasem Kamkar Rouhani¹, Hoshang Asadi-Haroni²

¹ Faculty of Mining, Petroleum and Geophysics, University of Shahrood, Shahrood, Iran

² Mining Faculty, Isfahan University of Technology, Isfahan, Iran

^{*}Corresponding author, e-mail: hssn.shahi@gmail.com

(received: 11/07/2014 ; accepted: 08/12/2014)

Abstract

The analysis of geochemical data in frequency domain, as indicated in this research study, can provide new exploratory information that may not be exposed in spatial domain. To identify deep geochemical anomalies, sulfide zone and geochemical noises in Dalli Cu–Au porphyry deposit, a new approach based on coupling Fourier transform (FT) and principal component analysis (PCA) has been used. The relationship between frequency attributes of surface geochemical data and mineralizing depth has been discussed. To determine the exploratory features in different frequencies, high- and low-pass filters have been performed on frequency domain; PCA method has been employed on these frequency bands separately. The results of this study have identified the mineralizing elements and showed the relationship between high- and low-frequencies and depths of anomalies. The geochemical halos of mineral deposits at different depths affected frequency distribution of elements in the surface. The information obtained from geophysical studies and exploration drillings, such as, trenches and boreholes, confirm the results of FT–PCA method. This new approach is very effective tool to identify the promising anomalies and deep mineralization without drilling.

Keywords: Principal component analysis (PCA), frequency domain, geochemical noises, two dimensional Fourier transformation.

Introduction

The geochemical interpretations are carried out in spatial domain. In addition to spatial domain methods for anomaly separation, the frequency domain of geochemical data were used to decompose the complex geochemical patterns and separate the background component that is related to very-low frequencies from anomalous factors (e.g., Zuo, 2011a,b; Hassani *et al.*, 2009; Cheng and Zhao, 2011; Cheng *et al.*, 2000; Cheng, 1999; Cao and Cheng, 2012; Afzal *et al.*, 2012).

The processing of geoscience data in frequency domain often involves operations, such as, filtering and reducing the noise from signal (Ge *et al.*, 2005). The spatial domain responses can be considered as superimposed signals of different frequencies (Cheng *et al.*, 2000). The spatial data can be transferred to the frequency domain based on two dimensional Fourier transformations (2DFT) (Cheng *et al.*, 1999; Cheng, 2006), which decomposes the signals to different frequencies. One of the equations for calculating the FT is presented by Dobrin and Savit (1988):

$$F(K_x, K_y) = \int_{-\infty}^{\infty} \int_{-\infty}^{\infty} f(x, y) \cos(K_x x + K_y y) dx dy$$

$$-i \int_{-\infty}^{\infty} \int_{-\infty}^{\infty} f(x, y) \sin(K_x x + K_y y) dx dy \quad (1)$$

where $f(x, y)$ is the signal in spatial domain, K_x and K_y are “wave numbers” with respect to the x and y axes. Wave number is the spatial counterpart of frequency increasing proportionally to wavelengths as follows:

$$\lambda_x = 2\pi / K_x, \quad \lambda_y = 2\pi / K_y, \quad (2)$$

$$\lambda = 2\pi \sqrt{(1/K_x^2 + 1/K_y^2)}$$

Therefore, $f(x, y)$ in the spatial domain, such as, geochemical map can be converted into $F(K_x, K_y)$. It consists of real and imaginary parts $R(K_x, K_y)$ and $I(K_x, K_y)$. The power spectrum is defined based on the following equation (Bhattacharyya, 1966; Gonzalez and Woods, 2002):

$$E(K_x, K_y) = R^2(K_x, K_y) + I^2(K_x, K_y) \quad (3)$$

Most of the studies in frequency domain have been performed on wave numbers or wavelengths and few studies have reported on the spatial distribution of the power spectrum (Cheng *et al.*, 2000).

The frequency domain have power spectrum values and wave numbers in directions of x and y , instead of elements geochemical map.

The filter function, $G(K_x, K_y)$, can modify the functions $R(K_x, K_y)$ and $I(K_x, K_y)$ by multiplying so that some ranges of wave numbers can be eliminated and others enhanced (Cheng *et al.*,

2000). Therefore, the filter function represents the decomposed functions and patterns of signals in certain frequencies being enhanced and others eliminated. It can be applied to geochemical anomaly separation.

The conventional filters in physics, electrical engineering, and geophysics, including low-pass, high-pass, band pass, and directional band pass filters (Cheng *et al.*, 2000). A low-pass filter generally eliminates the signals with high frequencies and a high-pass filter eliminates low frequencies. These filters may be performed on $K_x - K_y$ map only based on the wave number values without considering the power-spectrum values (e.g., Cheng and Xu, 1998).

In this study, to determine the exploratory features of geochemical data from Dalli area in different frequencies, high-pass and low-pass filters have been performed on frequency domain of geochemical data, based on wave number values. PCA method has been employed on these different frequency bands separately and as a result, mineralization components have been evaluated.

To investigate the characteristics of mineralization and identify the mineralization factor(s), PCA method has been frequently applied for analysis of geochemical and geoscience data (e.g. Chandrjith *et al.*, 2001; Garrett & Grunsky, 2001; Davis, 2002; Cheng *et al.*, 2006). PCA is a

multivariate statistical method for geo-information identification and integration of geo-datasets (Cheng *et al.*, 2011). Correlated variables in geo-datasets with high dimensionality are transformed into several non-correlated principal components, PCs, based on a covariance, or correlation matrix (Loughlin, 1991). The resultant reduced number of PCs increases the interpretability of the information for specific objectives (Zhao *et al.*, 2012).

Geology, alteration and mineralization of the study

Significant Cu porphyry deposits of Iran are related to calc-alkaline stocks in Sahand-Bazman, which is part of Urmia-Dokhtar intrusive-volcanic belt (Hezarkhani 2006a,b; Hou *et al.*, 2009). Dalli deposit is a part of this belt (Darabi-Golestan *et al.*, 2013), which is located in the Central Province of Iran (Asadi Haroni, 2008).

The mineralized Cu- Au zone in the study area is formed in the igneous diorite, quartz diorite porphyry and volcanic rocks, such as porphyritic amphibole, andesite, dacite and pyroclastics during the late Miocene to Pliocene (Fig. 1) (Darabi-Golestan *et al.*, 2013; Asadi Haroni, 2008).

Based on the regional geology, the volcanic (porphyritic amphibole andesite, and dacite) and pyroclastic rocks in the study area are associated with Late Miocene stratovolcanic rocks.

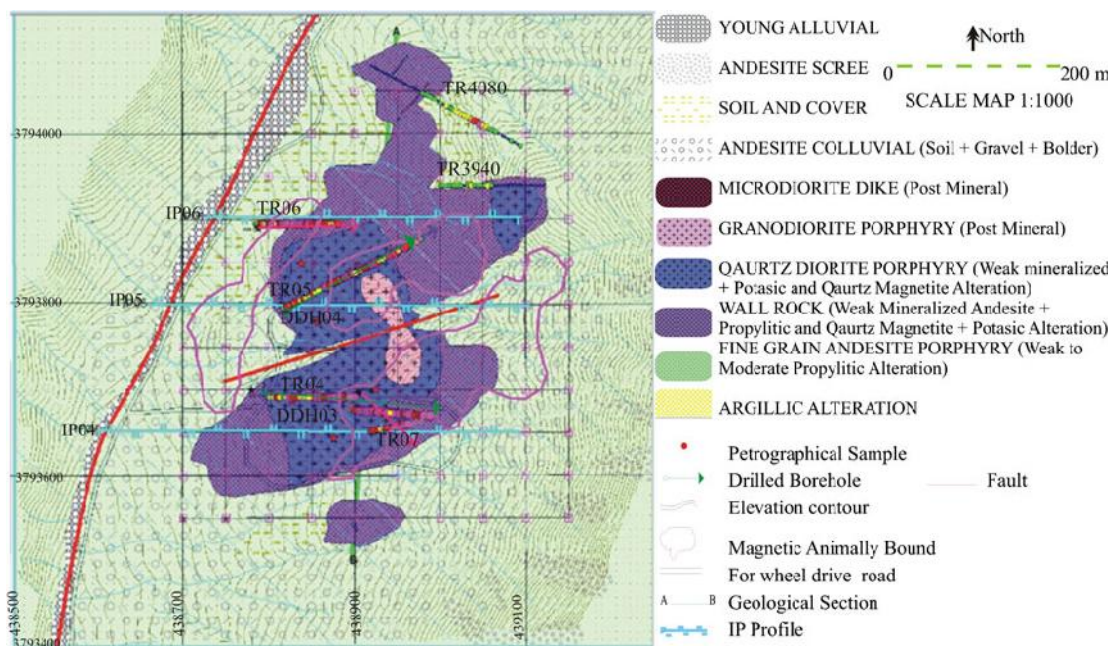


Figure 1. Local geological map of the Northern Dalli area showing the location of exploration survey (scale 1:1,000) (Asadi Haroni, 2008)

These are disposed with 30km in N-NE direction. Mineralization in Northern Dalli occurs in granodiorite plutonic complex (tonalite), quartz diorite, and andesitic rocks. Potassic alteration is formed during the tonalitic intrusion that contains high mineralization which includes quartz–potassium, feldspar–magnetite, and biotite.

The alteration zone in the study area covers an area of about 0.5 km. Potassic alteration is in the center of area and is progressively surrounded by sericitic, sericite–chlorite and propylitic assemblages towards the border in porphyry deposits. In andesite and quartz diorite porphyry rocks, Cu–Au mineralization is related to potassic–phyllic and propylitic–silicic alteration, respectively (Darabi-Golestan *et al.*, 2013). Magnetite is predominant mineral in the potassic zone, while sericite and chlorite minerals occur less in this zone (Hezarkhani *et al.*, 1999).

Discussion

The systematic soil sampling with a grid net of 50 × 50 m² has been used. One hundred sixty-five samples, with size fraction of –200 mesh, have been collected from the study area. The soil samples have been analyzed for 30 elements using inductively coupled plasma mass spectrometry (ICP-MS) method.

The spatial-domain geochemical data for 30 elements have been transferred to frequency-domain using 2DFT. The data in the frequency domain include the wave numbers in the directions of x and y, and their power spectrum values. The power spectrum map, created from the Mo content values, has been shown to illustrate the application of high- and low-pass filters and distribution of power spectrum. High values of power spectrum are mainly distributed around the center of the map corresponding to low frequencies. In general, the power-spectrum values decrease, moving away from the center (Fig. 2).

The high-frequency values represent great changes of concentration, whereas lower frequency values show little changes of concentration in geochemical distribution maps. The different geological processes can cause a variety of frequency attributes. Hence, in some complicated geological environments, extraction of exploratory features in spatial domain may be too difficult, while these patterns can be obtained in frequency domain. In this method, the relationship between

frequency attributes and mineralizing depth has been described. To survey the mineralization features and determine the elements related to mineralizing phase in different frequency bands, a newly developed approach based on coupling 2DFT and PCA was proposed. Therefore, three frequency bands have been considered and then high-pass and low-pass filters have been performed on frequency domain of geochemical data, based on wave number values; then PCA method has been employed on these different frequency bands separately. As a result, mineralization components have been evaluated in each frequency band.

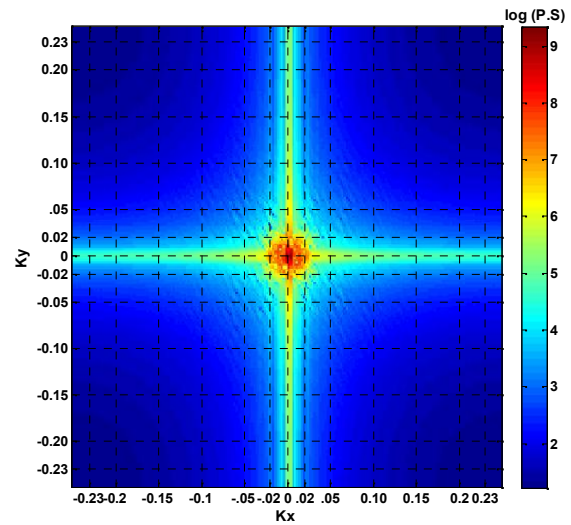


Figure 2. Mo power-spectrum (P.S) map obtained by two-dimensional Fourier transformation (2DFT)

Frequency band 1:

The power spectrums with wave numbers more than 0.20 have been selected. Therefore, high-pass filter has been used, based on wave number values in Equation 4, to preserve the high frequencies and delete the frequency inside rectangular box (Fig. 3).

The filter function, $G(K_x, K_y)$, modify the function $E(K_x, K_y)$ by multiplying so that some ranges of wave numbers are eliminated and others enhanced.

$$G(k_x, k_y) = \begin{cases} 1 & |k_x| \geq 0.20 \quad \text{OR} \quad |k_y| \geq 0.20 \\ 0 & \text{otherwise} \end{cases} \tag{4}$$

PCA method has been performed on this frequency band and the results are shown in Table

1 and Figure 6. The high frequencies in the power spectrum map include the effects of geochemical noises. PCA has classified the frequency-domain geochemical data into three components. The third principal component, which is recognized as

mineralization component, consists of elements Cu, Au, Cr, Ba, Ni, B, Ti, Ce, Co, K, La and Mn. Mineralization factor in this band represents the high-frequency anomaly, which is generally related to surface anomaly and geochemical noises.

Table 1. Rotated component matrix in PCA method on frequency-domain of geochemical data

	Principal components frequency band 1 in				Principal components frequency band 2 in		Principal components frequency band 3 in		
	1	2	3		1	2	1	2	
Au	.106	.210	.970	Au	.459	.833	Au	.868	.212
Al	.901	.151	.220	Al	.943	.332	Al	.990	.136
As	.182	.897	.371	As	.911	.412	As	.986	.169
B	.348	.361	.862	B	.932	.361	B	.990	.141
Ba	.084	.215	.966	Ba	.939	.343	Ba	.992	.123
Ca	.151	.932	.314	Ca	.866	.476	Ca	.982	.133
Ce	.286	.431	.847	Ce	.943	.331	Ce	.990	.137
Co	.291	.764	.567	Co	.942	.336	Co	.990	.138
Cr	.720	.179	.653	Cr	.938	.347	Cr	.989	.148
Cu	.197	.423	.876	Cu	.571	.786	Cu	.863	.359
Fe	.649	.685	.312	Fe	.943	.334	Fe	.991	.136
Ga	.803	.454	.372	Ga	.944	.330	Ga	.991	.135
K	.400	.013	.900	K	.942	.336	K	.991	.134
La	.425	.682	.586	La	.943	.331	La	.990	.136
Li	.835	.302	.453	Li	.938	.346	Li	.990	.137
Mg	.971	.176	.033	Mg	.944	.330	Mg	.991	.133
Mn	.849	.112	.509	Mn	.934	.356	Mn	.990	.143
Mo	.692	.669	.225	Mo	.076	.958	Mo	.113	.990
Na	.676	.686	.178	Na	.939	.343	Na	.991	.129
Ni	.721	.216	.639	Ni	.920	.392	Ni	.985	.174
P	.157	.975	.071	P	.944	.330	P	.990	.136
Pb	.629	.713	.268	Pb	.939	.343	Pb	.992	.126
S	.962	.179	.021	S	.499	.791	S	.917	.275
Sc	.247	.779	.071	Sc	.939	.342	Sc	.989	.149
Sr	-.002	.926	.370	Sr	.924	.381	Sr	.992	.122
Ti	.270	.618	.725	Ti	.938	.345	Ti	.991	.137
V	.714	.657	.131	V	.939	.342	V	.990	.141
Y	.374	.884	.245	Y	.944	.328	Y	.990	.136
Zn	.859	.227	.316	Zn	.943	.332	Zn	.991	.129
Zr	.859	.196	.165	Zr	.933	.360	Zr	.986	.164

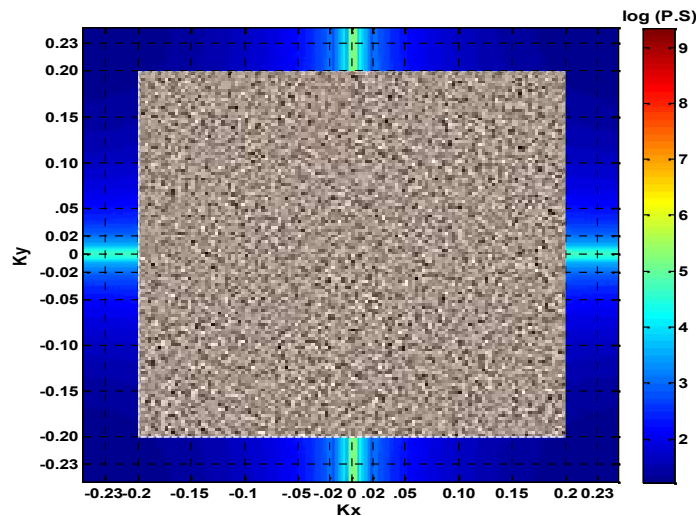


Figure 3. Mo power-spectrum (P.S) map obtained by applying Fourier transformation and high-pass filter on the geochemical data in frequency band 1.

The geochemical noises in high frequency data reduce the accuracy of results. Hence, FT-PCA approach on high frequencies has not separated the mineralizing elements of Au and Cu.

Mo is not classified in mineralization factor and not correlated with Cu and Au. The surface soil samples confirm these results and Mo has weak anomaly in the surface unlike Cu and Au.

Frequency band 2:

The power spectrums with wave numbers <0.05 have been selected. Therefore, low-pass filter has been used, based on wave number values in Equation 5, to preserve the low frequencies and delete the frequency outside of the rectangular box (Fig. 4).

$$G(k_x, k_y) = \begin{cases} 1 & |k_x|, |k_y| \leq 0.05 \\ 0 & \text{otherwise} \end{cases} \quad (5)$$

PCA method has been performed on this frequency band and the results have been shown in Table 1 and Figure 6. PCA classifies the 30 elements into two components. The second principal component, which is recognized as mineralization component, consists of elements Cu, Au, Mo and S. The low frequencies in the power spectrum map in this band do not have effects of geochemical noises; therefore, mineralization factor

is generally related to real anomaly. The results of FT-PCA approach on the frequency band 2 have identified the mineralizing elements of Au, Cu and Mo, and have shown the component of mineralization better than the results of the frequency band 1 (i.e., high frequencies in geochemical distribution of elements). The presence of S in the mineralization component can be related to the sulfide zone in subsurface. These results are confirmed with the results of boreholes and geophysical studies in the area. The distributions of Cu—Mo and Au in borehole DDH03 have shown in Figures 8 and 9, respectively. There are Cu, Au and Mo geochemical anomalies related to this mineralization deposit.

The six trenches TR04, TR05, TR06, TR07, TR3940, and TR4080 have been drilled in the area (Fig. 1). The results of rock sample analyses in these trenches confirmed that the results of the FT-PCA approach on the frequency band 2 showed the highest concentrations of Au and Cu in the contact of andesite and quartz diorite porphyry rocks.

Frequency band 3:

The power spectrums with wave numbers <0.0025 have been selected. Therefore, low-pass filter has been used, based on wave number values in

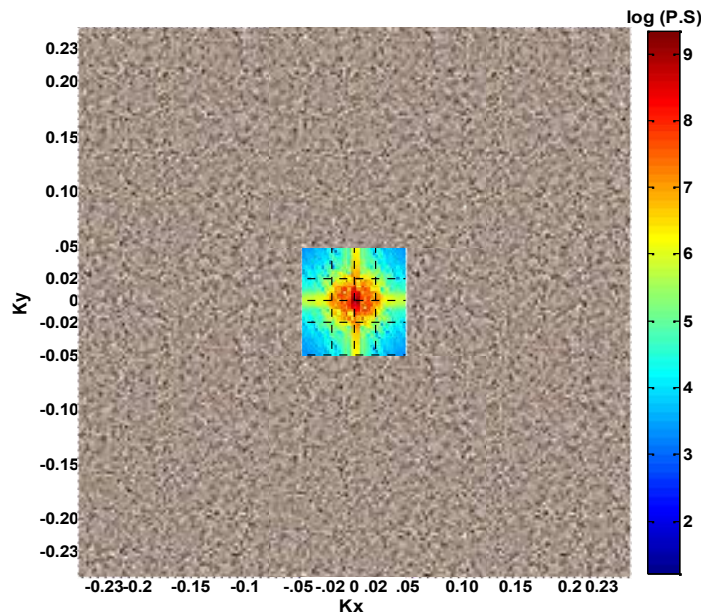


Figure 4. Mo power-spectrum (P.S) map obtained by applying Fourier transformation and high-pass filter on the geochemical data in frequency band 2.

Equation 6, to preserve very low frequencies and delete the frequency outside of the rectangular box (Fig. 5).

$$G(k_x, k_y) = \begin{cases} 1 & |k_x|, |k_y| \leq 0.0025 \\ 0 & \text{otherwise} \end{cases} \quad (6)$$

PCA method has been performed on this frequency band and the results are shown in Table 1 and Figure 6. PCA has classified the 30 elements into two components in this frequency band. Twenty-nine elements have been classified together in the first component and Mo has been in the second component, separately.

The low frequencies in the power spectrum map do not have effects of surface geochemical noises, while they can relate to background values and deep geochemical anomalies. The elements of first principal component (Table 1) have high similarity with frequency band 3 that includes very low frequencies, and relate to geochemical background values. The second principal component, in this frequency band (Table 1), that is recognized as mineralization component shows deep Mo geochemical anomaly. The mineralization component in frequency band 2 includes Cu, Au, Mo and S, while the mineralization component in frequency band 3 is only confined to Mo.

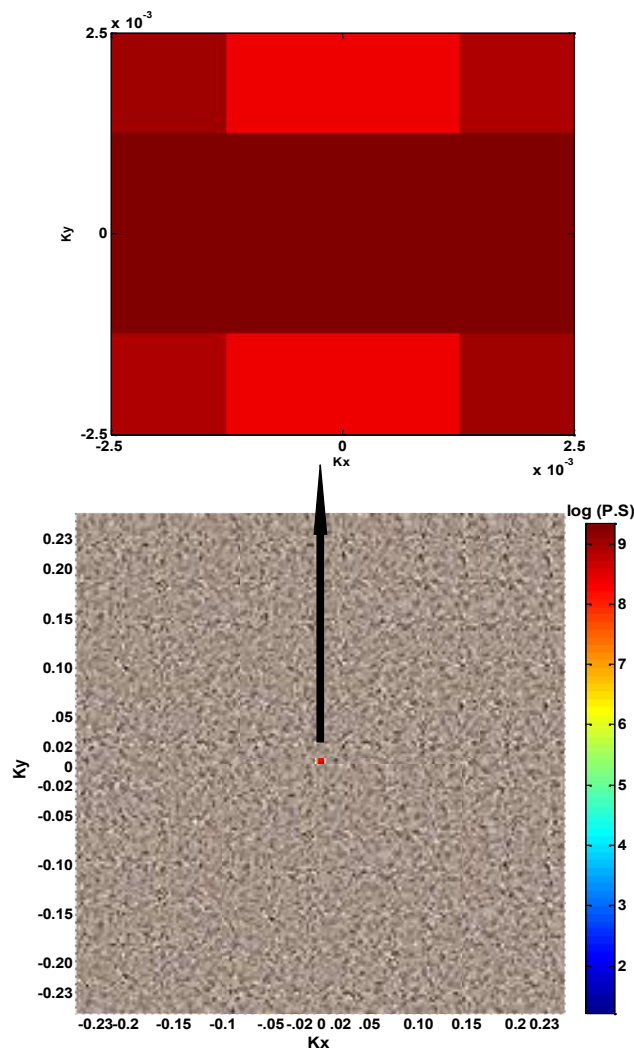


Figure 5. Mo power-spectrum (P.S) map obtained by applying Fourier transformation and high-pass filter on the geochemical data in frequency band 3.

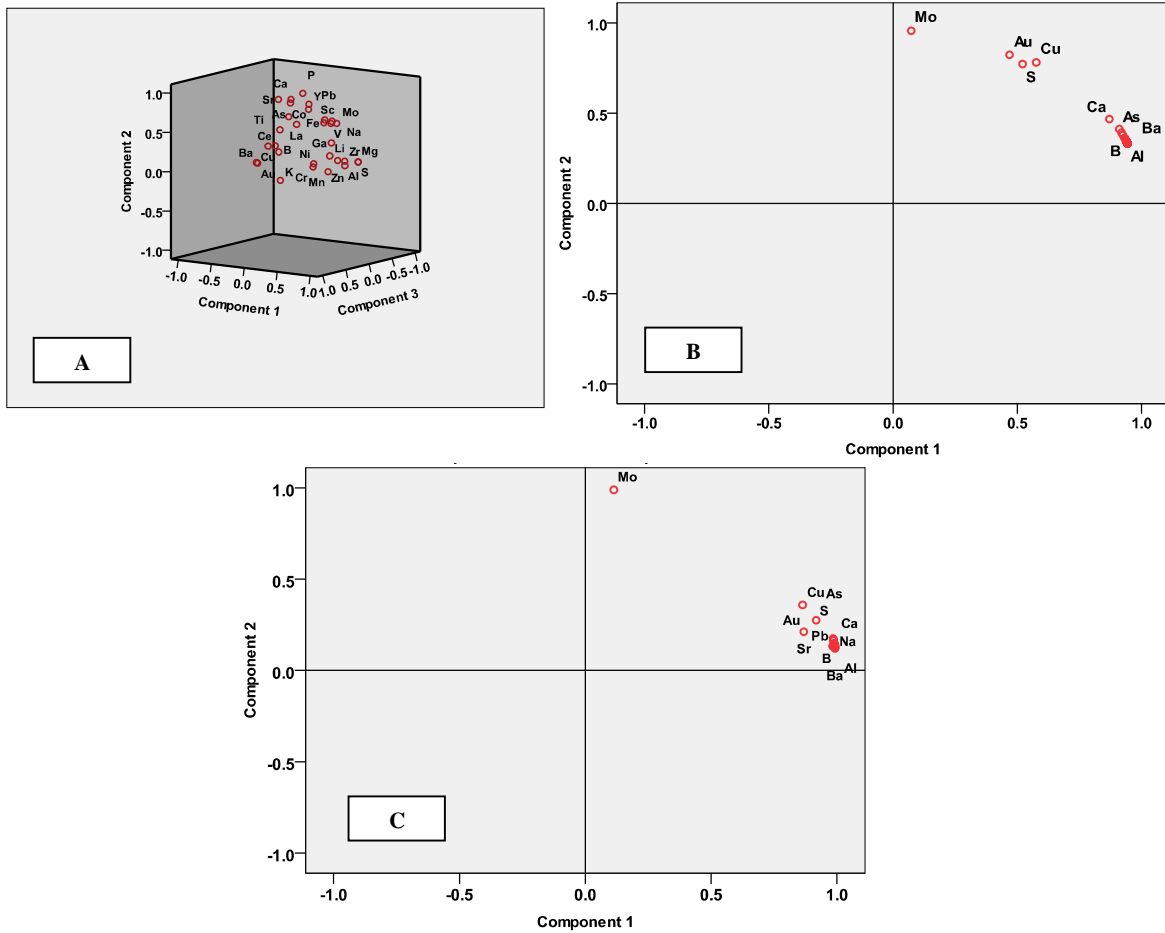


Figure 6. Component plot in rotated space using PCA on frequency-domain of geochemical data. A) frequency band 1, B) frequency band 2, and C) frequency band 3.

These results are confirmed with the results of borehole DDH03 in the area. Distributions of Cu-Mo and Au in this borehole are shown in Figures 8 and 9, respectively. In this borehole, Au and Cu have decreasing and Mo has increasing trend from surface to depth. There is a Mo geochemical anomaly from the depth of 240 m downward in this borehole (Figs. 8 and 9).

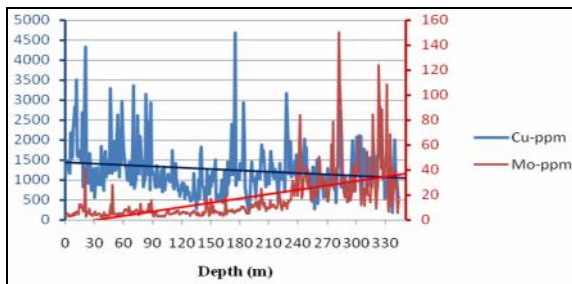


Figure 7. Variations of Mo -Cu values and their trends in borehole DDH03

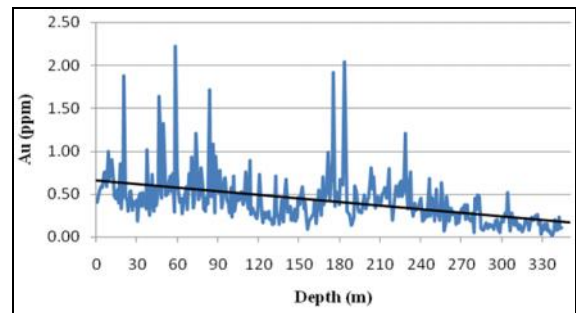


Figure 8. Variations of Au values and its decreasing trend in borehole DDH03

There is also a clear trend in the variations of Cu, Au, and Mo in the study area. Whatever gets away from the contact of andesite and quartz diorite porphyry, and wall rock (andesite rock) to the intrusive rock (granodiorite rock), the mineralization zone showed a sequential enrichment of Au - Cu - Mo.

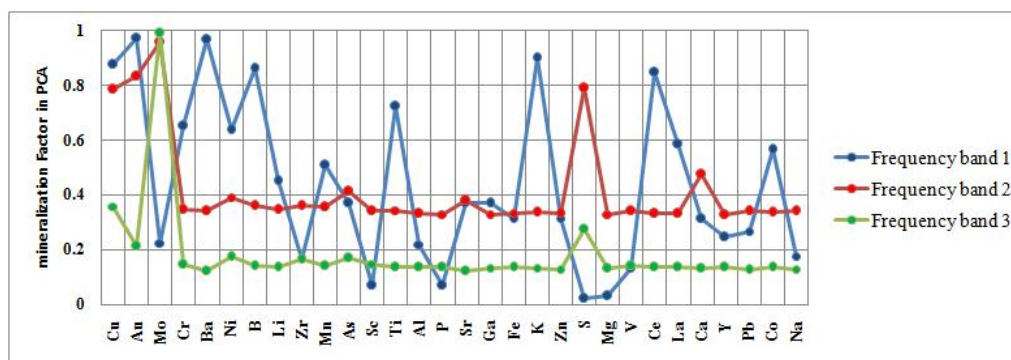


Figure 9. Comparison of PCA values of mineralization factors in frequency bands 1, 2 and 3

Figure 9 illustrates the PCA values of mineralization factor in FT-PCA method, and also, the numbers in Table 1 are the PCA values in frequency bands 1, 2 and 3. The principal components 3, 2, and 2 as mineralization factor in frequency bands 1, 2 and 3, respectively, have been shown in Table 1 and Figure 9. The elements related to mineralization process in different

frequency bands have been compared in this Figure. The Figure indicates, in frequency band 3, that includes very low frequencies, Mo has individually been in mineralization factor, while Cu and Au have been in background factor.

The final results of FT-PCA approach have been shown in Table 2.

Table 2. The final results of FT-PCA approach in frequency bands 1, 2 and 3

	Filter	Mineralization Factor
Frequency band-1	$G(k_x, k_y) = \begin{cases} 1 & k_x \geq 0.20 \quad \text{OR} \quad k_y \geq 0.20 \\ 0 & \text{otherwise} \end{cases}$ (High pass)	Cu, Au, Cr, Ba, Ni, B, Ti, Ce, Co, K, La, Mn
Frequency band-2	$G(k_x, k_y) = \begin{cases} 1 & k_x , k_y \leq 0.05 \\ 0 & \text{otherwise} \end{cases}$ (low pass)	Cu, Au, Mo, S
Frequency band-3	$G(k_x, k_y) = \begin{cases} 1 & k_x , k_y \leq 0.0025 \\ 0 & \text{otherwise} \end{cases}$ (low pass)	Mo

As the depth increases, the elements related to mineralization decrease, and deep Mo geochemical anomaly is separated from other elements at very low frequencies. Therefore, the very low frequency band is related to background values and deep geochemical anomaly, while the high-frequency anomaly is related to surface anomaly and geochemical noises.

Conclusion

To identify deep geochemical anomalies and detecting mineralization features in Dalli mineralization area, a newly developed approach

based on coupling Fourier transform and principal component analysis has been used. As a result, frequency-domain geochemical data have been separated into three frequency bands using high- and low-pass filters, and then, PCA technique has been performed on the data.

In frequency band 1, the power spectrums with wave numbers >0.20 have been selected, in which PCA has classified the frequency-domain geochemical data into three components. The third principal component, which consists of elements Cu, Au, Cr, Ba, Ni, B, Ti, Ce, Co, K, La and Mn, has been recognized as mineralization component.

This factor represents the high-frequency anomaly, which is related to surface anomaly and geochemical noises. FT-PCA approach on high frequencies has not separated the mineralizing elements of Au and Cu. In this frequency band, Mo has not been classified in mineralization factor.

In frequency band 2, the power spectrums with wave numbers >0.05 have been selected and PCA has classified the frequency-domain data into two components. The second principal component, which consists of elements Cu, Au, Mo and S, has been recognized as mineralization component. The sulfide zone has been cleared in this band that is related to relatively deep region. The low frequencies in the power spectrum map in this band do not have effects of geochemical noises; therefore, mineralization factor in this band is related to real anomaly. These results have been confirmed with the results of exploration drilling, or borehole data in the area.

In frequency band 3, the power spectrum values with wave numbers <0.0025 have been selected. In this frequency band, PCA has classified 30 elements into two components. Twenty-nine

elements have been classified in the first component and Mo has been in the second component individually. The low frequencies in the power spectrum map do not have effects of surface geochemical noises, while they can be related to background values and deep geochemical anomalies. The elements of first principal component have high similarity together in frequency band 3 and relate to geochemical background values. The second principal component that has been recognized as mineralization component shows deep Mo geochemical anomaly. The results of the FT-PCA approach have demonstrated that the very low frequency band is related to favorable rock types, background values and deep geochemical anomaly while the high-frequency anomaly is related to surface anomaly and geochemical noises. This approach represents the information from deep anomalies and mineralization trends, which is not achievable in spatial domain of surface geochemical data. The results have been confirmed with the results of exploration drilling in the area.

References

- Afzal, P., Fadakar Alghalandis, Y., Moarefvand, P., Rashidnejad Omran, N., Asadi Haroni, H., 2012. Application of power-spectrum-volume fractal method for detecting hypogene, supergene enrichment, leached and barren zones in Kahang Cu porphyry deposit, Central Iran, *Journal of Geochemical Exploration*, 112: 131-138.
- Asadi Haroni, H., 2008. First stage drilling report on Dalli porphyry Cu– Au prospect, Central Province of Iran, Technical Report.
- Bhattacharyya, B. K., 1966. Continuous spectrum of the total-magnetic-field anomaly due to a rectangular prismatic body. *Geophysics*, 31(1): 97-121.
- Cao, L., Cheng, Q., 2012. Quantification of anisotropic scale invariance of geochemical anomalies associated with Sn-Cu mineralization in Gejiu, Yunnan Province, China, *Geochemical Exploration*, 122: 47- 54.
- Chandrajith, R., Dissanayake, C.B., Tobschall, H.J., 2001. Application of multi-element relationships in stream sediments to mineral exploration: a case study of Walawe Ganga Basin, Sri Lanka. *Applied Geochemistry*, 16 (3): 339- 350.
- Cheng, Q., 1999. Spatial and scaling modelling for geochemical anomaly separation. *Journal of Geochemical Exploration*, 65: 175- 194.
- Cheng, Q., 2006. Multifractal modelling and spectrum analysis of gamma ray spectrometer data from southwestern Nova Scotia, Canada, *Science in China*, 49(3): 283-294.
- Cheng, Q., Xu, Y., Grunsky, E., 1999. Integrated spatial and spectral analysis for geochemical anomaly separation. In: Lippard, S.J., Naess, A., Sinding-Larsen, R. (Eds.), *Proceedings of the Fifth Annual Conference of the International Association for Mathematical Geology*, Trondheim, Norway 6–11th August, 1: 87- 92.
- Cheng, Q., Xu, Y., Grunsky, E., 2000. *Integrated Spatial and Spectrum Method for Geochemical Anomaly Separation*, Natural Resources Research, 9:1.
- Cheng, Q., Jing, L., Panahi, A., 2006. Principal component analysis with optimum order sample correlation coefficient for image enhancement. *International Journal of Remote Sensing*, 27 (16): 3387- 3401.
- Cheng, Q., Bonham-Carter, G., Wang, W., Zhang, S., Li, W., Xia, Q., 2011. A spatially weighted principal component analysis for multi-element geochemical data for mapping locations of felsic intrusions in the Gejiu mineral district of Yunnan, China. *Computer & Geosciences*, 37: 662- 669.
- Cheng, Q., Xu, Y., 1998. Geophysical data processing and interpreting and for mineral potential mapping in GIS environment. In *Proceedings of the Fourth Annual Conference of the International Association for Mathematical Geology*, 2: 394-399.

- Cheng, Q., Zhao, P., 2011. Singularity theories and methods for characterizing mineralization processes and mapping geo-anomalies for mineral deposit prediction. *Geoscience Frontiers*, 2(1): 67-79.
- Darabi-Golestan, F., Ghavami-Riabi, R., Asadi-Harooni, H., 2013. Alteration, zoning model, and mineralogical structure considering litho-geochemical investigation in Northern Dalli Cu–Au porphyry. *Arabian Journal of Geosciences*, 6(12): 4821-4831.
- Davis, J.C., 2002. *Statistics and Data Analysis in Geology*, 3rd ed., John Wiley & Sons Inc., New York, 550 pp.
- Dobrin, M. B., Savit, C. H., 1988. *Geophysical prospecting*: McGraw-Hill Book Co., New York, 867 p.
- Garrett, R.G., Grunsky, E.C., 2001. Weighted sums- knowledge based empirical indices for use in exploration geochemistry. *Geochemistry: Exploration Environment Analysis* 1, 135–141.
- Ge, Y., Cheng, Q., Zhang, S., 2005. Reduction of edge effects in spatial information extraction from regional geochemical data: a case study based on multifractal filtering technique, *Computers & Geosciences* 31: 545- 554.
- Gonzalez, R.C., Woods, R.E., 2002. *Digital image processing*. Prentice-Hall, Upper Saddle River, NJ, 793 pp.
- Hassani, H., Daya, A., Alinia, F., 2009. Application of a fractal method relating power spectrum and area for separation of geochemical anomalies from background. *Aust J Basic Appl Sci*, 3(4): 3307-3320.
- Hezarkhani, A., 2006a. Hydrothermal evolution of the Sar-Cheshmeh porphyry Cu–Mo deposit. Iran: evidence from fluid inclusions. *J Asian Earth Sci* 28: 409- 422
- Hezarkhani, A. 2006b. Petrology of the intrusive rocks within the Sungun porphyry copper deposit, Azerbaijan, Iran. *J Asian Earth Sci.*, 27: 326–340
- Hezarkhani, A., Williams-Jones, A. E., & Gammons, C. H., 1999. Factors controlling copper solubility and chalcopyrite deposition in the Sungun porphyry copper deposit, Iran. *Mineralium deposita*, 34(8): 770-783.
- Hou, Z., Yang, Z., Qu, X., Meng, X., Li, Z., Beaudoin, G., & Zaw, K., 2009. The Miocene Gangdese porphyry copper belt generated during post-collisional extension in the Tibetan Orogen. *Ore geology reviews*, 36(1): 25-51.
- Loughlin, W. P., 1991. Principal component analysis for alteration mapping. *Photogrammetric Engineering and Remote Sensing*, 57(9): 1163-1169.
- Zhao, J., Wang, W., Dong, L., Yang, W., & Cheng, Q., 2012. Application of geochemical anomaly identification methods in mapping of intermediate and felsic igneous rocks in eastern Tianshan, China. *Journal of Geochemical Exploration*, 122: 81-89.
- Zuo, R., 2011a. Identifying geochemical anomalies associated with Cu and Pb–Zn skarn mineralization using principal component analysis and spectrum–area fractal the Gangdese Belt, Tibet (China). *J. Geochemical Exploration*. 111: 13-22.
- Zuo, R., 2011b. Decomposing of mixed pattern of arsenic using fractal model in Gangdese belt, Tibet, China. *Applied Geochemistry*, 26: S271-S273.